

**Isolation of Taste-Active Triterpenoids from *Quercus*
robur: Sensory Assessment and Identification in Wines and
Spirit**

Marine Gammacurta,[†] Pierre Waffo-Teguo,[†] Delphine Winstel,[†] Denis Dubourdiou,[†] and Axel
Marchal^{*,†}

[†] Univ. Bordeaux, Unité de Recherche Œnologie, EA 4577, USC 1366 INRA, ISVV, 33882 Villenave
d'Ornon Cedex, France

ABSTRACT: Six new triterpenoids (**1–6**), two known genins (**7** and **8**), and five known functionalized triterpenoids (**9–13**) were isolated from a *Quercus robur* heartwood extract. The purification protocol was guided by LC-HRMS by searching for structural analogues of bartogenic acid on the basis of their putative empirical formula. The structures of the new compounds were unequivocally elucidated using HRESIMS and 1D/2D NMR experiments. Sensory analyses were performed in water and in a non-oaked white wine on the pure compounds **1–13** at 5 mg/L. All molecules were perceived as bitter in water and wine, but they were mostly reported as modifying the wine taste balance. Using LC-HRMS, compounds **1–13** were observed in oaked red wine and cognac and were semi-quantified in oak wood extracts. The influence of two cooperage parameters, oak species and toasting process, on compounds **1–13** content was studied. All compounds were found in quantities significantly higher in pedunculate than in sessile oak wood. Toasting is a key step in barrel manufacture and modulates the concentration of the discussed compounds. Significantly higher quantities were observed in untoasted wood compared to medium or highly toasted one. These findings provide new insights into the molecular origin of taste changes due to oak aging.

Food choices are influenced by a wide range of cultural, psychological, economic, practical, nutritional and sensory factors. Taste acceptability is the first condition for food intake. Among all the flavors perceived in food, bitterness is considered the least palatable. In fact, the bitter substances of plants are often toxic,¹ and disgust for these substances could be the result of an adaptation so that plant-eating species can survive.² While humans have only one sweetness receptor, they have 25 for bitterness and are able to detect a wide range of bitter compounds.³ Nevertheless, bitterness can also contribute to the complexity and palatability of certain foods. For instance, the quality of wine depends not only on its aromatic profile but also on its taste balance. This balance relies on a subtle combination of sour, sweet and bitter flavors⁴ and its perception in red wines can be modulated by their tannic structure.

From a molecular point of view, wine acidity is due to organic acids occurring in grapes or produced by fermentary micro-organisms.⁵ The bitterness of dry wines remains partly unexplained, as is the origin of the sweet flavor. It is indeed necessary to distinguish the sweet wines, defined by concentrations of glucose and fructose above their detection threshold, from the dry wines. In the latter, grape carbohydrates are almost completely consumed by yeasts, so they are present only at very low concentrations and are not perceptible. Despite the lack of residual sugars, dry wines commonly develop a sweet perception described by experts as "sweetness without sugar". The molecular bases of this phenomenon have been recently the scope of various works. Indeed, molecular markers of this perception have been identified in grapes⁶ as yeast autolysis products,⁷ and in oak wood.⁸ Indeed, most great wines and some spirits undergo aging before bottling. Aging is traditionally performed in oak barrels and two species are used in Europe: *Quercus petraea* (Matt.) Liebl. and *Quercus robur* L. (Fagaceae). In contact with oak wood, the sensory properties of wines and spirits are modified owing to the release of volatile and non-volatile compounds. For instance, sweet triterpenoids were recently identified in oak wood⁸⁻¹⁰ and explain the well-established gain of sweetness.¹¹ In addition to

this sweetening effect, contact with oak wood during aging can also lead to an increase in bitterness, which can affect the taste balance of wine. Glabasnia and Hofmann highlighted the bitter properties of some ellagitannins and established their detection thresholds.^{12,13} However, the concentrations observed in wines are below these thresholds, so their influence on taste is very weak or non-existent.¹⁴⁻¹⁶ More recently, the bitterness of several compounds released during oak wood aging such as lignans^{17,18} was highlighted. However, data linking chemical structures and sensory properties are sparse and most of the numerous non-volatile compounds identified in wine have not yet been characterized for their sensory properties. For these reasons, the molecular origin of the taste of wine remains largely unexplained.

Recently, several studies have focused on triterpenoids present in oak wood and especially quercotriterpenoside I (QTT I) and its isomers. These compounds derived from arjungenin significantly influence the taste balance of wine by increasing its sweetness.⁸⁻¹⁰ However, 28-*O*- β -D-glucopyranosyl bartogenic acid (Glu-BA) is a triterpene derived from bartogenic acid identified in oak wood¹⁹ and exhibiting a bitter taste.²⁰ As for QTT I, some Glu-BA isomers or derivatives might occur in oak wood that could have similar taste properties. In this study, such structural analogues to Glu-BA were sought by LC-HRMS in oak wood extracts, wine and spirit. Empirical formulas of potential isomers were calculated, and Fourier transform mass spectrometry coupled with UHPLC was used to perform targeted screening. This analytical technique was also used to guide the purification of target compounds, and structural elucidation was achieved by NMR spectroscopy. The identification of new taste markers in oak wood is of importance since it paves the way for practical applications for better monitoring of the aging of wine and spirits.

RESULTS AND DISCUSSION

Chips of *Q. robur* heartwood were macerated in an H₂O–EtOH solution (40:60; v/v). The first step consisted of sequential liquid/liquid extraction using MTBE and EtOAc to obtain pre-purified extracts. The resulting enriched MTBE extract was subjected to centrifugal partition chromatography (CPC), yielding 10 fractions. Preparative HPLC of fraction I gave two new triterpenoids (**1** and **2**) and two known triterpenoids (**10** and **11**). The EtOAc extract was also subjected to CPC, yielding three fractions (I to III). Preparative HPLC of fraction I gave two new triterpenoids (**3** and **4**) and two known triterpenoids (**12** and **13**). Fraction II was still complex, so another liquid/liquid extraction using *n*-BuOH was performed followed by solid phase extraction (SPE) and preparative HPLC. This yielded two new triterpenoids (**5** and **6**) and one known triterpenoid (**9**). Finally, a second CPC was carried out on fraction III, followed by preparative HPLC to obtain two known genins (**7** and **8**).

Analysis of HRESIMS and NMR spectroscopic data indicated that compounds **3–6**, **9**, and **12** and **13** contain at least one sugar unit. The ¹³C NMR chemical shifts of the glycoside part suggested that it was a glucose moiety. All the vicinal coupling constants of the hexosyl moiety of all isolated compounds were of 7-8 Hz magnitude (Table 1; Table S1, Supporting Information), indicating a β -glucopyranose structure. Supportive GC-MS analysis of the hydrolysate extract of a mixture of compounds **3–6**, **9**, and **12–13** demonstrated that glucose was the only sugar unit detectable. To prove the absolute configuration of the glucose, GC-MS analysis was performed after chiral derivatization.²¹ The respective thiazolidine derivatives were compared to two standard sugars: D- and L-glucose. These experiments demonstrated that the sugar moieties of all isolated compounds were all D-glucose.

The negative-ion HRESIMS of compound **1** showed a deprotonated molecular ion [M – H][–] at *m/z* 669.3286 (Figure S1, Supporting Information). Given the isotopic ratio (around 41% abundance of ¹³C isotope), the empirical formula of compound **1** was determined as C₃₇H₅₀O₁₁. To investigate the nature and the sequence of the functional groups, fragmentation

was performed on the pure molecule by non-resonant activation in the higher collision dissociation (HCD) mode with a 90 arbitrary unit collision energy. The presence of an ion at m/z 517.3163 ($[C_{30}H_{45}O_7]^-$) corresponding to the loss of $C_7H_4O_4$ suggested that compound **1** contains one galloyl group (Figure S1, Supporting Information). This observation was confirmed by the presence of an ion at m/z 169.0134 ($[C_7H_5O_5]^-$) corresponding to gallic acid. Moreover, the empirical formula of the ion at m/z 517.3163 corresponded to a tetrahydroxyoleane-type triterpenoid.

The 1H and ^{13}C NMR data of **1** (Tables 1 and 2) were similar to those previously described for compound **10**,²² but with some differences in ring A. The ^{13}C NMR spectrum showed 30 carbon signals due to a triterpenoid moiety and seven to a galloyl unit. Careful analysis of the 1D and 2D NMR spectra [1H , COSY, ROESY, HSQC-TOCSY, HSQC, and HMBC (Figures S2 and S3, Supporting Information)] suggested the presence of a signal at δ_C 203.7 (proton at δ 10.10 typical for a formyl group proton), a carboxylic acid signal at δ_C 180.9, two olefinic carbons at δ_C 143.3 and 124.6, three oxymethines at δ_C 81.1, 76.8, and 66.5, oxymethylene at δ_C 58.3, and five singlets corresponding to tertiary methyl groups characteristic of a polyhydroxyoleanane-type triterpenoid (Table 2). Based on the comparison with ^{13}C NMR data (Table 2) previously reported in the literature,²² the triterpenoid part of the compound **1** was identified as robural A [$2\alpha,3\beta,19\alpha,23$ -tetrahydroxy-24-oxo-olean-12-en-28-oic acid]. The relative configuration of the triterpenoid was confirmed by a ROESY experiment (Figure 1; Figure S2, Supporting Information). The formyl group is located at C-24 instead of C-23 due to the roe effect between the H-24 at δ_H 10.10 ppm and H-2 at δ_H 4.36 ppm; H-24 and H-25 at 0.96 ppm; and H-2 and H-25. According to the mass spectrum of compound **1**, a galloyl group was connected to the triterpenoid moiety. The galloyl unit was confirmed by the presence of a singlet signal integrated for two protons at δ_H 7.08 (H-2'''/6''') in the 1H NMR spectrum. In addition six aromatic carbons at δ_C 120.1 (C-1'''), 109.0 (C-2'''/ C-6'''), 145.2 (C-3'''/ C-5'''), 138.5

(C-4'''), together with an esterified carboxyl carbon at δ_C 167.1 (C-7'''), finally confirmed the presence of a galloyl moiety. The HMBC correlation between H-3 at δ_H 5.20 of the triterpenoid moiety and δ_C 167.1 (C-7''') of the galloyl unit revealed that the galloylation occurred at C-3 of robural A. Compound **1** was shown to be regioisomer of **10** with a gallate linked to C-3 rather than to C-23 (Figure 1). Thus, the structure of compound **1** was elucidated as 3-*O*-galloyl robural A.

The molecular formula of compound **2** was deduced as C₃₇H₅₀O₁₁ based on the HRESIMS ([M – H][–] *m/z* 669.3281), which corresponds to a trihydroxyoleane-type triterpenoid with a galloyl moiety (Figure S4, Supporting Information). The ¹H and ¹³C NMR data of compound **2** (Tables 1 and 2) were closely comparable to those of 3-*O*-galloyl bartogenic acid previously published in the literature,²² except for the presence of a carboxylic acid group at δ_C 175.8 located at the C-23 position rather than at C-24. This was in agreement with the ROE effect between H-2 at δ_H 4.59 and Me-24 at δ_H 1.25 (Figure 1), suggesting that the triterpenoid part in compound **2** was barrinic acid [(2 α ,3 β ,4 β ,19 α)-2,3,19-trihydroxyolean-12-ene-23,28-dioic acid]. The galloyl unit was linked to C-3 of the triterpenoid moiety, as indicated by the HMBC cross-peak between the proton at δ_H 4.74 (H-3) and the carbon (C-7''') at δ_C 167.6 of the gallate group. The structure of compound **2** was determined therefore as 3-*O*-galloyl barrinic acid.

Compound **3** showed a negative-ion HRESIMS quasi molecular ion peak at *m/z* 831.3798 (Figure S7, Supporting Information). Its empirical formula was determined as C₄₃H₆₀O₁₆. The ion at *m/z* 517.3157 was detected in the fragmentation spectrum of the pure molecule by non-resonant activation in the HCD mode. It corresponded to the loss of C₁₃H₁₄O₉ and its empirical formula (C₃₀H₄₆O₇) was assigned to a trihydroxyoleane-type triterpenoid. This suggested that compound **3** contains one hexosyl and one galloyl group (Figure S7, Supporting Information). This observation was supported by the presence of another peak related to the ion

m/z 679.3684 ($[C_{36}H_{55}O_{12}]^-$) and corresponding to the loss of $C_7H_4O_4$, suggesting that compound **3** contains one galloyl group.

The ^{13}C NMR showed 43 carbon signals of which 30 were assigned to a triterpenoid moiety, seven to a galloyl unit, and six to a hexosyl group. The resonance signals due to the triterpenoid moiety in the ^{13}C NMR spectrum of compound **3** (Table 2) included two carboxylic acid groups at δ_C 180.7 (C-28) and 176.8 (C-24), two olefinic carbons at δ_C 143.1 (C-13) and 123.5 (C-12), three oxymethines at δ_C 93.2 (C-3), 81.15 (C-19) and 65.6 (C-2), and five singlets at δ_C 22.2 (C-23), 13.3 (C-25), 16.2 (C-26), 26.9 (C-29) and 23.4 (C-30), corresponding to tertiary methyl groups. By comparing chemical shifts with those described previously,²³ the triterpenoid moiety of compound **3** was identified as bartogenic acid [$2\alpha,3\beta,19\alpha$ -trihydroxyolean-12-en-24,28-dioic acid]. The relative configuration was confirmed by a ROESY experiment. As shown from the MS, the hexosyl group is connected to the triterpenoid moiety. Complete assignments of the glycosidic proton system were achieved using 1H - 1H COSY and HMBC-TOCSY experiments. The HMBC experiment showed cross-peaks between C-3 at δ_C 93.2 of bartogenic acid and H-1' at δ_H 4.39 and between C-7''' at δ_C 166.4 of the gallate group and H-6' α δ_H 4.37 and H-6' β at δ_H 4.62. Thus, the structure of compound **3** was determined as 3-*O*-[(6-*O*-galloyl)- β -D-glucopyranosyl] bartogenic acid.

The molecular formula of compound **4** was established by negative HRESIMS ($[M - H]^-$ m/z 831.3795) as $C_{43}H_{60}O_{16}$, again corresponding to a tetrahydroxyoleane-type triterpenoid with a hexosyl moiety and a galloyl moiety (Figure S10, Supporting Information). The fragment ion at m/z 313.0560 ($[C_{13}H_{13}O_9]^-$) indicated that these moieties are linked. The presence of fragment ions at m/z 169.0132 ($[C_7H_5O_5]^-$) and m/z 679.3688 ($[C_{36}H_{55}O_{12}]^-$) suggested that the galloyl group was in a terminal position. The 1H and ^{13}C NMR data of compound **4** (Tables 1 and 2) showed similarities to those described for compound **3**, but with some slight differences in ring A. The carboxylic acid group was located at C-23 instead of C-24 based on the ROE

effect between H-2 at δ_{H} 4.42 and H-24 at δ_{H} 1.51 of the triterpenoid moiety. Therefore, the structure of **4** was established as 3-*O*-[(6-*O*-galloyl)- β -D-glucopyranosyl] barrinic acid.

The negative-ion HRESIMS of compound **5** showed a deprotonated molecular ion $[\text{M} - \text{H}]^-$ at m/z 993.4313 (Figure S13, Supporting Information). Its empirical formula was determined as $\text{C}_{49}\text{H}_{70}\text{O}_{21}$. Fragment ions were observed at m/z 831.3790 ($[\text{C}_{43}\text{H}_{59}\text{O}_{16}]^-$), at 679.3686 ($[\text{C}_{36}\text{H}_{55}\text{O}_{12}]^-$) and at 517.3160 ($[\text{C}_{30}\text{H}_{45}\text{O}_7]^-$) and corresponded to the loss of one hexosyl group, one hexosyl and one galloyl group, and of two hexosyl and one galloyl groups, respectively. Moreover, fragment ions were also observed at m/z 313.0558 ($[\text{C}_{13}\text{H}_{13}\text{O}_9]^-$) and at m/z 169.0131 ($[\text{C}_7\text{H}_5\text{O}_5]^-$), indicating a hexose-galloyl moiety. The presence of a fragment ion at m/z 841.4210 ($[\text{C}_{42}\text{H}_{65}\text{O}_{17}]^-$), corresponding to the loss of a galloyl group, suggested that the latter could be in the terminal position, meaning not linked to two other moieties. The ^{13}C NMR spectrum revealed 49 carbon signals, of which 30 were attributed to the triterpenoid moiety, 12 to the two hexosyl groups, and seven to the galloyl unit. Analysis of the NMR spectra [^1H , ^{13}C , COSY, ROESY, HSQC-TOCSY, HSQC, and HMBC (Figures S14 and S15, Supporting Information)] demonstrated that the triterpenoid moiety of **5** is bartogenic acid. Analysis of the 2D NMR experiment (COSY, ROESY, HSQC-TOCSY) allowed two sugars to be assigned as β -glucopyranosyl ester (δ_{H} 5.38, δ_{C} 94.2) linked to C-28 of bartogenic acid, and glucopyranosyl ether (δ_{H} 4.39, δ_{C} 105.2) attached to the C-3 of the triterpenoid part of **5**. Moreover, the sugar linked in C-3 of the triterpenoids was found to possess a deshielded H-6 α at (δ_{H} 4.39) and H-6 β at (δ_{H} 4.62), indicating the location of the galloyl unit. This was confirmed by HMBC and ROESY NMR experiments. Thus, the structure of compound **5** was established as 3-*O*-[(6-*O*-galloyl)- β -D-glucopyranosyl]-28-*O*-[β -D-glucopyranosyl] bartogenic acid.

The molecular formula of compound **6** was deduced by negative HRESIMS ($[\text{M} - \text{H}]^-$ m/z 993.4302) as $\text{C}_{43}\text{H}_{62}\text{O}_{15}$. Fragment ions were observed at m/z 841.4296 ($[\text{C}_{42}\text{H}_{65}\text{O}_{17}]^-$), 831.3792 ($[\text{C}_{43}\text{H}_{59}\text{O}_{16}]^-$), 679.3685 ($[\text{C}_{36}\text{H}_{55}\text{O}_{12}]^-$), 517.3159 ($[\text{C}_{30}\text{H}_{45}\text{O}_7]^-$), and 313.0557

($[\text{C}_{13}\text{H}_{13}\text{O}_9]^-$) (Figure S16, Supporting Information). These data suggested that compound **6** is composed of a tetrahydroxyoleane-type triterpenoid with a hexose-galloyl moiety and a hexosyl group. The ^1H and ^{13}C NMR data of compound **6** (Tables 1 and 2) showed similarities to those of **5**, but with some slight differences in ring A. The carboxyl group was located at C-23 instead of C-24 based on the ROE correlation between H-2 at δ_{H} 4.45 and H-24 at δ_{H} 1.61 of the triterpenoid moiety, indicating that the triterpenoid part is barrinic acid. The structure of **6** was established therefore as 3-*O*-[(6-*O*-galloyl)- β -D-glucopyranosyl]-28-*O*-[β -D-glucopyranosyl] barrinic acid.

The negative-ion HRESIMS of compounds **7–13** showed a deprotonated molecular ion $[\text{M} - \text{H}]^-$ at m/z 517.3184, 517.3182, 679.3709, 669.3774, 669.3779, 831.3834, and 831.3818, respectively. Considering the mass accuracy specifications of the spectrometer and the isotopic ratio observed (35, 35, 41, 42, 42, 48, and 48% for the ^{13}C -containing isotope, respectively), the empirical formula, $\text{C}_{30}\text{H}_{46}\text{O}_7$, was assigned to compounds **7** and **8**, $\text{C}_{36}\text{H}_{56}\text{O}_{12}$ to compound **9**, $\text{C}_{37}\text{H}_{50}\text{O}_{11}$ to compounds **10** and **11**, and $\text{C}_{43}\text{H}_{59}\text{O}_{16}$ to compounds **12** and **13**. The NMR data (Table S1 and S2, Supporting Information) and specific optical rotation (+41, +55, +22, +11, +11, -8, +20) of each compound were compared to literature data. Compounds **7** and **8** appeared to be barrinic acid and bartogenic acid, respectively. Compound **7** was identified for the first time in *Barringtonia acutangula*,²⁴ while compound **8** was observed in *Vochysia vismiaefolia*,²³ then in *Q. robur* and *Q. petraea* by Arramon et al.¹⁹ Compound **9** was identified as another glucosyl derivative of bartogenic acid named 2 α ,3 β ,19 α -trihydroxyolean-12-ene-23,28-dioic acid 28-*O*- β -D-glucopyranoside (Glu-BA II), observed once in *B. acutangula* seeds,²⁵ but never in the genus *Quercus*. Compounds **10** and **11** were found to be a galloyl derivative of robural A and bartogenic acid, named 23-*O*-galloyl robural A and 2-*O*-galloyl bartogenic acid, respectively. They were identified recently in *Q. robur*.²² Finally, compounds **12** and **13** were determined as isomers of compounds **3** and **4** named 3-*O*-galloyl bartogenic acid 28-*O*- β -D-

glucopyranosyl ester and 2-*O*-galloyl bartogenic acid 28-*O*- β -D-glucopyranosyl ester, respectively. They were observed recently for the first time in *Q. robur*.^{22,26} However, none of these compounds have been observed in an alcoholic beverage and their taste has not yet been described.

Since tasting is a destructive form of analysis and because the available quantities of the isolated compounds were limited, it was not possible to use a large panel of tasters to characterize the tastes of these compounds. Consequently, five experts were selected according to their level of experience in sensory analysis and gustative perception. Their expertise and training in wine tasting allowed them to perceive the potential differences between a model solution or a wine and the same sample supplemented with the purified compounds. Thus, all compounds were dissolved in water and in a non-oaked white wine (Bordeaux 2013) at 5 mg/L, and the taste of each solution was characterized in comparison with the blank water or the wine as a reference. The score indicated in Table 3 results from a consensus between the five experts. Glu-BA, an isomer of compound **9**, for which the bitter taste has already been documented,²⁰ was also tasted in the same session. It was perceived as slightly bitter in water (1/5) by the panelists. The same condition (5 mg/L in water) was applied to compounds **1–13**. On a 0–5 scale representing bitterness intensity, nine compounds (**1–2**, **5–7**, **9** and **11–13**) exhibited a bitter taste (Table 3). Compound **1** scored 1/5, compounds **7**, **9** and **11–13** scored 2/5, compound **2** scored 3/5, and compounds **5** and **6** were perceived intensively (4/5). These purified compounds were also supplemented in a non-oaked white wine in order to study their influence on wine taste (Table 3). The blank wine before any supplementation was scored 1/5 for sweetness and bitterness and 5/5 for acidity. The wine spiked with Glu-BA (5 mg/L) was described as more bitter (3/5), while the perception of acidity and sweetness was slightly unchanged. Compounds **3** and **10** were described as having no taste effect on the reference wine. Compounds **6–7** and **12** were perceived as strongly bitter in wine (5/5 for **6** and **7**; 4/5 for

12) without modifying the perception of acidity or sweetness. On the other hand, compounds **2**, **5**, and **9** were perceived as strongly bitter (5/5 for **2** and **5**; 4/5 for **9**), but the perception of acidity in wine was modified as their intensity decreased (scored 3/5). Compounds **4** and **11** slightly modified the bitterness of the wine (3/5) but strongly decreased sourness (scored 3/5 for **4**, 2/5 for **11**). Finally, the addition of compounds **1**, **8** and **13** in wine completely changed its taste balance by slightly increasing its bitterness (scored 2/5 for all) and sweetness (scored 2/5, 3/5, and 3/5, respectively) and by decreasing its acidity (scored 3/5, 2/5, and 2/5, respectively). Almost all compounds were perceived as more bitter in wine than in water. These results are in agreement with several studies that have underlined the importance of sensory interactions in the perception of taste and the role of matrix effects. In particular, they demonstrate the influence of ethanol and its ability to impart the perception of bitterness.²⁷⁻²⁹ Furlan et al. suggested that the interaction of flavanols with lipids present in the human bolus and in the buccal membranes could modulate the perception of both astringency and bitterness in wines.³⁰

This study is the first to highlight the taste properties of compounds **1–13** isolated from oak wood extracts. Some of the compounds were far more bitter than Glu-BA, so this approach is valid for obtaining better knowledge of taste markers present in oak wood. Nevertheless, these molecules are not transferred systematically from oak wood barrels to wine or spirits. Their transfer depends on their physico-chemical properties. To determine the potential impact of the taste-modifying compounds identified in this study, their presence in a commercial wine and a commercial cognac aged in oak barrels was investigated.

LC-HRMS is a powerful technique for screening and quantifying compounds in a complex matrix and was used previously to identify and quantitate oak^{10,18,31,32} and grape seed compounds³³ in wines and spirits. Its mass measurement accuracy allows the screening of m/z ions in a narrow window. By using LC-HRMS screening jointly with the comparison of

retention times and HCD fragmentation spectra, the presence of a given compound in a complex matrix may be confirmed. Figure 2 shows extracted ion chromatograms (XIC) obtained from an oak wood extract (left), an oaked red wine (middle), and an oaked cognac (right) for m/z ratios specific to compounds **1** to **13**. Similar signals were detected for all compounds in the three matrixes. Retention time similarity (<0.10 min) and specificity of mass measurement (<5 ppm) demonstrated that compounds **1–13** were present in oaked wine and cognac. In addition, the analyses of HCD fragmentation products revealed the same main fragment ions in the three matrices for each compound at the same retention time, which supported these conclusions.³⁴ Finally, the XIC corresponding to the purified compounds exhibited additional peaks that were not referenced in this study. Except for the peak at 3.02 min (m/z 679.3709), which can be assigned to Glu-BA from a comparison with the retention time of the pure compound, the others suggested the occurrence of minor isomers in oak wood, wine and cognac.

Next, the concentrations of compounds **1** to **13** were estimated in 35 samples of sessile oak wood and 34 samples of pedunculate oak wood. To compare the levels measured in samples of each species, statistical analysis was applied to quantitative data. Figure 3 shows the amounts of compounds **1** to **13** expressed in $\mu\text{g/g}$ of equivalent Glu-BA. For all compounds, the average concentration was higher in pedunculate than in sessile oak wood with significant differences for compounds **1–3**, **5–11** and **13**. These results were consistent with previous observations regarding the influence of oak species on the triterpenoid composition of oak wood. More arjungenin and its derivatives and isomers were observed in sessile oak wood than in pedunculate oak wood,^{10,20} whereas Glu-BA was more abundant in pedunculate when compared with sessile oak wood.²⁰ Although statistical tests revealed significant differences in the mean concentrations of almost all compounds, some extreme values of individual triterpenes were very close between sessile and pedunculate oak. Indeed, high inter-individual variations were observed within species for each triterpenoid, as shown by the large confidence

intervals. Therefore, the individual quantitation of each triterpenoid did not allow the direct identification of the botanical species. This limitation can be linked with observations concerning other compounds for which the concentrations depend on botanical species such as β -methyl- γ -octalactone³⁵ and ellagitannins.³⁶ To overcome this issue, Marchal et al. proposed calculating the base 10 logarithm of the ratio between the sum of concentrations in QTT I, II, and III and the concentration in Glu-BA for the unambiguous discrimination of oak species.²⁰ The new compounds identified in this study could also be used to assign the botanical species of oak by a chemical method.

In cooperage, several stages are necessary for the manufacture of barrels. Toasting is one of the most fundamental since it involves several modifications of the chemical composition of the barrels.³⁷⁻⁴⁰ Figure 4 shows the variations in the concentrations of compounds **1** to **13** according to toasting in pedunculate oak wood extracts. The results show a significant influence of toasting on the concentration of all molecules ($p < 0.05$). For all compounds, higher concentrations were observed in untoasted wood (UW) than in medium-toasted (MTW) or highly toasted (HTW) wood. Moreover, high toasting led to a significant decrease in triterpenoid contents, especially in compounds **1-4** and **8-13**. The same results were observed in sessile oak wood extracts (data not shown). The influence of toasting on the concentration of volatiles such as *cis*- and *trans*-methyloctalactone and vanillin⁴¹ and non-volatile compounds occurring in oak wood such as ellagitannins⁴² is well known. The present findings extend knowledge of the practical parameters likely to affect oak wood composition and the sensory properties of wine. The influence of the species of oak wood and the effect of toasting on the content of new triterpenoids has been established. Monitoring of these parameters might allow the concentrations of compounds **1-13** to be modulated, thus providing better control over the bitter contribution of barrel aging.

In conclusion, six new compounds (**1–6**) and two known isomers (**7** and **9**) have been identified for the first time in oak wood. The presence and taste of all the compounds in wine and spirit have also been established. Some of these exhibit a bitter taste in water, but their impact on wine taste balance was perceived more strongly, which suggests that they act as taste modifiers. Their real impact on wine taste requires the establishment of a detection threshold linked to quantification studies. They are also relevant markers of the oak species. These findings provide new insights into the molecular phenomena associated with barrel aging and offer promising perspectives for industrial applications related to oak wood selection and toasting in the cooperage industry.

EXPERIMENTAL SECTION

General Experimental Procedures. Optical rotations were measured with a JASCO P-2000 polarimeter. The sodium emission wavelength was set at 589 nm and the temperature at 293 K. The samples were dissolved in MeOH, and the final value resulted from a mean of 10 measurements of 10 s each. NMR experiments were conducted on a Bruker Avance 600 NMR spectrometer (^1H at 600 MHz and ^{13}C at 150 MHz) equipped with a 5 mm TXI probe. All 1D (proton) and 2D (COSY, ROESY, HMBC, and HSQC) spectra were acquired at 300 K in methanol- d_4 , which gave the solvent signal (^1H δ 3.31; ^{13}C δ 49.0) as reference. Data analysis was performed with Bruker Topspin version 3.2. The LC-HRESIMS platform consisted of an HTC PAL autosampler (CTC Analytics AG, Zwingen, Switzerland), an Accela UHPLC system with quaternary pumps, and an Exactive Orbitrap mass spectrometer equipped with a heated electrospray ionization (H-ESI) probe (both from Thermo Fisher Scientific, Bremen, Germany). CPC was performed on a Spotprep II LC paired with a SCPC-100 + 1000 (Armen Instrument, Saint-Avé, France), both controlled by Armen Glider Prep V5.0 software. SPE was used to purify some complex CPC fractions with an Oasis® HLB 20 cc Vac Cartridge (1 g sorbent per

cartridge, 60 μm particle size, 20/pk, Waters) with a vacuum manifold. A Waters Prep 150 LC including a 2545 Quaternary Gradient Module and a 2489 UV/visible detector was used for the last steps of purification. Final purification of compounds was performed by preparative HPLC using columns chosen after LC-HRMS tests. Therefore, a Hypersil Gold™ C₁₈ column (250 \times 21.2 mm, 5 μm particle size, Thermo Fisher Scientific) equipped with a preparative guard cartridge (20 \times 20 mm, 5 μm particle size, Thermo Fisher Scientific) was used to purify compounds 1–13. For LC-HRMS analyses and quantitation, a Hypersil Gold™ C₁₈ column (100 \times 2.1 mm, 1.9 μm particle size, Thermo Fisher Scientific) was used as stationary phase. Concerning hydrolysis, all GC-MS analyses were carried out on an Agilent 5975B Series GC/MSD System equipped with an Agilent 7683B autosampler, and Agilent 6890N GC System using a SGE BP20 (30 m \times 250 μm \times 0.25 μm) capillary column as stationary phase. Sample preparation, extraction, centrifugal partition chromatography, solid-phase extraction and high-performance liquid chromatography were performed with ultrapure water (Milli-Q purification system, Millipore, France) and HPLC grade solvents (VWR International, Pessac, France). LC-HRMS chromatographic separations were performed with LC-MS grade CH₃CN and deionized ultrapure water (Optima, Fisher Chemical, Illkirch, France). Two commercial wines were used in this study: a non-oaked white Bordeaux 2013 (100% Sauvignon Blanc, 12.5% v/v) for sensory analysis and a red Pessac-Léognan 2016 (60% Cabernet Sauvignon, 40% Merlot, 13.5% v/v) aged in new oak barrels for chemical analysis. A commercial brandy (Cognac XO) aged in oak barrels was also analyzed.

Plant Material. Oak wood used in this study was supplied by the cooperage company Seguin-Moreau (Merpins, France) as indicated in a previous study.¹⁰

Extraction and Isolation. The oak wood material (1 kg) was macerated in 4 L of H₂O–EtOH solution (40:60; v/v) for 2 weeks at room temperature. Filtration (0.45 μm) was used to remove wood chips and particles. The liquid medium was concentrated in vacuo to

remove EtOH and, partly, water. The aqueous solution (800 mL) was extracted successively with methyl *tert*-butyl ether (MTBE) (6 × 400 mL) and EtOAc (8 × 160 mL). The organic layers of each extraction step were combined, evaporated under reduced pressure, suspended in water and freeze-dried. The MTBE (1.8 g), the EtOAc (6 g), and the H₂O extracts (10 g) were stored under air- and light-protective conditions.

The MTBE extract was fractionated with a CPC using the Arizona solvent systems (*n*-heptane/EtOAc/MeOH/H₂O) H (1:3:1:3 v/v) and G (1:4:1:4 v/v). Only the lower phase (LPH) and the upper phase (UPH) of system H and the upper phase of system G (UPG) were used. The system was filled first with LPH (1200 rpm, 30 mL/min for 40 min), then equilibrated with UPH (1200 rpm, 30 mL/min for 55 min). Elution was performed as follows: 100% UPH (1200 rpm, 30 mL/min, 0–66 min), 0–100% UPG (1200 rpm, 30 mL/min, 66–100 min), 100% UPG (1200 rpm, 30 mL/min, 100–145 min), 100% LPH (1200 rpm, 50 mL/min, 145–190 min). Ten fractions were obtained (Fr. I–Fr. X). The MTBE extract was fractionated by one CPC run of 1.8 g injection.

Compound **1** (3.9 mg, $t_R = 17.1$ min), compound **2** (5.7 mg, $t_R = 23.7$ min), compound **10** (2.1 mg, $t_R = 13.3$ min), and compound **11** (2.6 mg, $t_R = 26.7$ min) were purified from CPC fraction I (224 mg) by preparative HPLC (H₂O/CH₃CN, both acidified with 0.05% TFA) with a gradient at 20 mL/min as follows: 35% B (0–7 min), 35–50% B (7–42 min), 50–100% B (42–44 min).

The EtOAc extract was fractionated with a CPC using the Arizona solvent system G (*n*-heptane/EtOAc/MeOH/H₂O, 1:4:1:4 v/v) to obtain three fractions (Fr. I– Fr. III). The EtOAc extract was fractionated by three consecutive CPC runs, with an average of 1.9 g by injection.

Compound **3** (7.2 mg, $t_R = 18.2$ min), compound **4** (37.1 mg, $t_R = 36$ min), compound **11** (1.5 mg, $t_R = 14.1$ min), and compound **12** (1 mg, $t_R = 23.6$ min) were purified from CPC fraction I (100 mg) by preparative HPLC (H₂O/CH₃CN, both acidified with 0.05% TFA) with

a gradient at 20 mL/min as follows: 25% B (0–7 min), 25–35% B (7–37 min), 35–40% B (37–40 min), 40–100% B (40–42 min).

The CPC fraction II containing compounds **5**, **6** and **9** was still abundant (700 mg) and chemically complex. Fraction II was dissolved in water and a liquid/liquid extraction was carried out using *n*-BuOH (1 × 250 mL). The organic layer was then evaporated under reduced pressure, suspended in water and freeze-dried. The *n*-BuOH extract (240 mg) was purified by SPE. A series of MeOH/H₂O acidified with TFA (0.05%) solutions (10, 50, 60, 80, and 100%) was used to elute compounds **5**, **6** and **9**. Final purification of compounds was performed by preparative HPLC using ultrapure H₂O (solvent A) and CH₃CN (solvent B), both acidified with 0.05% TFA. The 60% SPE fraction (57.7 mg) containing compound **5** (2.2 mg, *t_R* = 10 min) and compound **6** (5.5 mg, *t_R* = 28.1 min) was eluted with a gradient at 20 mL/min as follows: 25% B (0–7 min), 25–40% B (7–37 min), 40–100% B (37–39 min). Compound **9** (2.2 mg, *t_R* = 29.5 min) present in the 80% SPE fraction (57.1 mg) was purified using a gradient 20 mL/min as follows: 25% B (0–7 min), 25–35% B (7–22 min), 35% B (22–37 min), 35–100% B (37–39 min).

Finally, compounds **7** and **8** were present in the chemically complex CPC fraction III (1.5 g). Thus, a second CPC was performed using the Arizona solvent system L (*n*-heptane/AcOEt/MeOH/H₂O, 2.5:3:2.5:3 v/v) providing eight fractions (Fr. A–Fr. H). Compound **7** (5.7 mg, *t_R* = 18.1 min) and compound **8** (126 mg, *t_R* = 20.2 min) were purified from Fr. B by preparative HPLC (H₂O/CH₃CN both acidified with 0.05% TFA) using a gradient 20 mL/min as follows: 35% B (0–7 min), 35–40% B (7–45 min), 40–100% B (45–46 min).

All CPC extract and preparative HPLC experiments were performed as previously described.¹⁰ Concerning preparative HPLC, elution was monitored by UV detection at 280 nm and by evaporative light scattering detection (ELSD) for compounds **7** and **8**, which were not

detected at 280 nm. Samples obtained after successive injections were pooled, evaporated in vacuo to remove acetonitrile and freeze-dried twice to obtain white amorphous powders.

3-O-Galloyl robural A (1): white, amorphous powder; $[\alpha]^{25}_D +30$ (*c* 0.1, MeOH); ^1H NMR (methanol-*d*₄, 600 MHz) and ^{13}C NMR (methanol-*d*₄, 150 MHz), see Tables 1 and 2; (–)-HRMS *m/z* 669.3286 (calcd for C₃₇H₄₉O₁₁[–], 669.3269).

3-O-Galloyl barrinic acid (2): white, amorphous powder; $[\alpha]^{25}_D +40$ (*c* 0.1, MeOH); ^1H NMR (methanol-*d*₄, 600 MHz) and ^{13}C NMR (methanol-*d*₄, 150 MHz), see Tables 1 and 2; (–)-HRMS *m/z* 669.3281 (calcd for C₃₇H₄₉O₁₁[–], 669.3269).

3-O-[(6-O-galloyl)-β-D-glucopyranosyl] bartogenic acid (3): white, amorphous powder; $[\alpha]^{25}_D +24$ (*c* 0.1, MeOH); ^1H NMR (methanol-*d*₄, 600 MHz) and ^{13}C NMR (methanol-*d*₄, 150 MHz), see Tables 1 and 2; (–)-HRMS *m/z* 831.3798 (calcd for C₄₃H₅₉O₁₆[–], 831.3798).

3-O-[(6-O-galloyl)-β-D-glucopyranosyl] barrinic acid (4): white, amorphous powder; $[\alpha]^{25}_D +3$ (*c* 0.1, MeOH); ^1H NMR (methanol-*d*₄, 600 MHz) and ^{13}C NMR (methanol-*d*₄, 150 MHz), see Tables 1 and 2; (–)-HRMS *m/z* 831.3795 (calcd for C₄₃H₅₉O₁₆[–], 831.3798).

3-O-[(6-O-galloyl)-β-D-glucopyranosyl]-28-O-[β-D-glucopyranosyl] bartogenic acid (5): white, amorphous powder; $[\alpha]^{25}_D -5$ (*c* 0.1, MeOH); ^1H NMR (methanol-*d*₄, 600 MHz) and ^{13}C NMR (methanol-*d*₄, 150 MHz), see Tables 1 and 2; (–)-HRMS *m/z* 993.4313 (calcd for C₄₉H₆₉O₂₁[–], 993.4326).

3-O-[(6-O-galloyl)-β-D-glucopyranosyl]-28-O-[β-D-glucopyranosyl] barrinic acid (6): white, amorphous powder; $[\alpha]^{25}_D +6$ (*c* 0.1, MeOH); ^1H NMR (methanol-*d*₄, 600 MHz) and ^{13}C NMR (methanol-*d*₄, 150 MHz), see Tables 1 and 2; (–)-HRMS *m/z* 993.4302 (calcd for C₄₉H₆₉O₂₁[–], 993.4326).

Barrinic acid (7): white, amorphous powder; $[\alpha]^{25}_D +41$ (*c* 0.1, MeOH); ^1H NMR (methanol-*d*₄, 600 MHz) and ^{13}C NMR (methanol-*d*₄, 150 MHz), see Tables S1 and S2, Supporting Information; (–)-HRMS *m/z* 517.3171 (calcd for C₃₀H₄₅O₇[–], 517.3160).

Bartogenic acid (8): white, amorphous powder; $[\alpha]^{25}_{\text{D}} +55$ (*c* 0.1, MeOH); ^1H NMR (methanol-*d*₄, 600 MHz) and ^{13}C NMR (methanol-*d*₄, 150 MHz), see Tables S1 and S2, Supporting Information; (–)-HRMS *m/z* 517.3174 (calcd for C₃₀H₄₅O₇[–], 517.3160).

2 α ,3 β ,19 α -trihydroxyolean-12-ene-23,28-dioic acid 28-O- β -D-glucopyranoside (9): white, amorphous powder; $[\alpha]^{25}_{\text{D}} +22$ (*c* 0.1, MeOH); ^1H NMR (methanol-*d*₄, 600 MHz) and ^{13}C NMR (methanol-*d*₄, 150 MHz), see Tables S1 and S2, Supporting Information; (–)-HRMS *m/z* 679.3704 (calcd for C₃₆H₅₅O₁₂[–], 679.3688).

23-O-Galloyl robural A (10): white, amorphous powder; $[\alpha]^{25}_{\text{D}} +11$ (*c* 0.1, MeOH); ^1H NMR (methanol-*d*₄, 600 MHz) and ^{13}C NMR (methanol-*d*₄, 150 MHz), see Tables S1 and S2, Supporting Information; (–)-HRMS *m/z* 669.3274 (calcd for C₃₇H₄₉O₁₁[–], 669.3269).

2-O-Galloyl bartogenic acid (11): white, amorphous powder; $[\alpha]^{25}_{\text{D}} +11$ (*c* 0.1, MeOH); ^1H NMR (methanol-*d*₄, 600 MHz) and ^{13}C NMR (methanol-*d*₄, 150 MHz), see Tables S1 and S2, Supporting Information; (–)-HRMS *m/z* 669.3279 (calcd for C₃₇H₄₉O₁₁[–], 669.3269).

3-O-Galloyl bartogenic acid 28-O- β -D-glucopyranosyl ester (12): white, amorphous powder; $[\alpha]^{25}_{\text{D}} -8$ (*c* 0.1, MeOH); ^1H NMR (methanol-*d*₄, 600 MHz) and ^{13}C NMR (methanol-*d*₄, 150 MHz), see Tables S1 and S2, Supporting Information; (–)-HRMS *m/z* 831.3834 (calcd for C₄₃H₅₉O₁₆[–], 831.3798).

2-O-Galloyl bartogenic acid 28-O- β -D-glucopyranosyl ester (13): white, amorphous powder; $[\alpha]^{25}_{\text{D}} +20$ (*c* 0.1, MeOH); ^1H NMR (methanol-*d*₄, 600 MHz) and ^{13}C NMR (methanol-*d*₄, 150 MHz), see Tables S1 and S2, Supporting Information; (–)-HRMS *m/z* 831.3818 (calcd for C₄₃H₅₉O₁₆[–], 831.3798).

Hydrolysis and Derivatization Procedure. A mixture of 1 mg of compounds **3–6**, **9**, and **12** and **13** was refluxed with 10 mL 2 N HCl for 2 h. The mixture was extracted with EtOAc (3 \times 15 mL). The aqueous phase was neutralized with 0.5 M KOH and freeze-dried. The dried hydrolysate (1 g) was derivatized with L-cysteine methyl ester hydrochloride (7.5 g/L in

pyridine, 4 mL, 60 °C, 1 h), subsequently silylated with *N,O*-bis(trimethylsilyl)trifluoroacetamide and chlorotrimethylsilane (BSTFA-TMCS = 99:1, v/v; 500 µL, 60 °C, 1 h) and analyzed by GC-MS. Reference compounds (purity ≥99.5%, Sigma-Aldrich) D-glucose 0.9 mg (t_R = 33.70 min) and L-glucose 1.2 mg (t_R = 34.50 min) were derivatized and analyzed using the same protocol. The following GC-MS parameters were applied: oven 100 °C for 1 min, then 5 °C/min to 250 °C for 15 min, total run time 52 min; injection volume 2 µL; splitless; carrier gas helium; flow rate 1 mL/min; SCAN mode.

Sensory Analysis. Compounds 1–13 were submitted to sensory analyses as described in a previous study.¹⁰ Briefly, the purified compounds were dissolved at 5 mg/L in water (eau de source de Montagne, Laqueuille, France), and in a non-oaked white wine (Bordeaux, 2013). The panelists were asked to describe the taste perception of each compound using the vocabulary of winetasting. Bitterness, sweetness, and acidity intensity were evaluated on a scale from 0 (not detectable) to 5 (strongly detectable) compared to a blank solution (water and wine). Glu-BA, identified by Arramon et al.¹⁹ and tasted for the first time by Marchal et al.,²⁰ was used as the bitter reference.

Quantitation of Compounds 1 to 13 by LC-HRMS. Quantitation was performed using the LC-HRESIMS method described in a previous study.¹⁰ First, the influence of oak wood species on triterpene contents was determined on oak wood extracts (n = 35 for sessile oak wood, n = 34 for pedunculate oak wood) provided and prepared by the barrel manufacturer (Seguin Moreau) as described in a previous study.²⁰ Then, in order to study the influence of toasting on triterpene content, 10 staves of each species were prepared by the barrel manufacturer (Seguin Moreau) and provided untoasted (UW, n = 10 for each species), medium-toasted (MTW, n = 10 for each species), and highly toasted (HTW, n = 10 for each species). Medium and highly toasted corresponds to oak wood toasted at 180 °C for 30 min and at 200 °C for 4 h, respectively. Untoasted wood samples came from the outer face of the staves,

medium-toasted ones were collected on the inner side after toasting, and the rest of the staves were heated in an oven, i.e., highly toasted. Such sampling avoids artefacts due to high inter-individual variability. Then, samples were ground into powders and macerated in a wine model solution (H₂O/EtOH: 88/12, 5 g/L tartaric acid, pH 3.5) at 50 g/L for 48 h. They were then diluted five times with Milli-Q water and filtered through a 0.45 µm PTFE syringe filter before being injected. Oak wood species (sessile or pedunculate) were determined with the method developed by Guichoux et al.⁴³ Quantities of compounds were too low to build calibration curves. Thus, the results were expressed as µg/g (of oak wood) equivalent Glu-BA, on the basis of the dilution factor. For this purpose, a calibration curve was first built by injecting increasing concentrations of Glu-BA, as described in a previous study.²⁰ Then, for the samples, the peaks corresponding to each analyte were integrated. The equation obtained from the calibration curve of Glu-BA was applied to the areas in order to calculate the concentrations of each purified compound.

Statistical Analysis. All values are expressed as mean ± 95% confidence interval (CI). The normal distribution was tested and revealed that the data don't follow a normal distribution. Thus, statistical analysis was performed using the Kruskal–Wallis test followed by the post hoc Dunn test and XL-STAT version 2019.1.1.56334 (Addinsoft, Paris, France).

ASSOCIATED CONTENT

Supporting Information

The following data are available as Supporting Information:

NMR spectroscopic data for compounds **7–13**. HRMS spectra of compounds **1–6** in the full-scan and HCD mode. 1D (¹H) and 2D (COSY, ROESY, HSQC and HMBC) NMR spectra of **1–6**.

AUTHOR INFORMATION

Corresponding Author

E-mail: axel.marchal@u-bordeaux.fr. Tel +33557575867

ORCID

Marine Gammacurta: 0000-0002-3802-5161

Delphine Winstel: 0000-0002-1967-6540

Axel Marchal: 0000-0002-4053-2998

Notes: The authors declare no competing financial interests.

ACKNOWLEDGMENTS

The authors are very grateful to Dr. A. Prida and Dr. J.-C. Mathurin for providing samples.

They also thank Dr. Ray Cooke for proofreading the manuscript and Dr Warren Albertin for statistical interpretation. This work was funded by Seguin-Moreau, Rémy Martin, Biolaffort, the Conseil Interprofessionnel des Vins de Bordeaux and France AgriMer.

REFERENCES

- (1) Nissim, I.; Dagan-Wiener, A.; Niv, M. Y. *IUBMB Life* **2017**, *69*, 938–946.
- (2) Xue, A. Y.; Di Pizio, A.; Levit, A.; Yarnitzky, T.; Penn, O.; Pupko, T.; Niv, M. Y. *Front. Mol. Biosci.* **2018**, *5*, 9.
- (3) Dagan-Wiener, A.; Di Pizio, A.; Nissim, I.; Bahia, M. S.; Dubovski, N.; Margulis, E.; Niv, M. Y. *Nucleic Acids Res.* **2019**, *47* (Database issue), D1179–D1185.
- (4) Peynaud, E. *Knowing and Making Wine*; Wiley: New York, 1981.
- (5) Ribéreau-Gayon, P.; Dubourdieu, D.; Donèche, B.; Lonvaud, A. *Handbook of Enology, Vol. 7, 7th Ed., Microbiology of Wine*; Dunod: Paris, 2019.
- (6) Cretin, B. N.; Waffo-Teguo, P.; Dubourdieu, D.; Marchal, A. *Food Chem.* **2019**, *272*, 388–395.
- (7) Marchal, A.; Marullo, P.; Durand, C.; Moine, V.; Dubourdieu, D. *J. Agric. Food Chem.* **2015**, *63*, 2364.
- (8) Marchal, A.; Waffo-Téguo, P.; Génin, E.; Mérillon, J.-M.; Dubourdieu, D. *Anal. Chem.* **2011**, *83*, 9629–9637.
- (9) Marchal, A.; Génin, E.; Waffo-Téguo, P.; Bibès, A.; Da Costa, G.; Mérillon, J.-M.; Dubourdieu, D. *Anal. Chim. Acta* **2015**, *853*, 425–434.
- (10) Gammacurta, M.; Waffo-Teguo, P.; Winstel, D.; Cretin, B. N.; Sindt, L.; Dubourdieu, D.; Marchal, A. *J. Nat. Prod.* **2019**, *82*, 265–275.
- (11) Marchal, A.; Pons, A.; Lavigne, V.; Dubourdieu, D. *Aust. J. Grape Wine Res.* **2013**, *19*, 11–19.
- (12) Glabasnia, A.; Hofmann, T. *Agric. Food Chem.* **2006**, *54*, 3380–3390.
- (13) Stark, T.; Wollmann, N.; Wenker, K.; Lösch, S.; Glabasnia, A.; Hofmann, T. *J. Agric. Food Chem.* **2010**, *58*, 6360–6369.

- (14) Chira, K.; Zeng, L.; Le Floch, A.; Péchamat, L.; Jourdes, M.; Teissedre, P.-L. *Tetrahedron* **2015**, *71*, 2999–3006.
- (15) Masson, G.; Moutounet, M.; Puech, J. L. *Am. J. Enol. Vitic.* **1995**, *46*, 262–268.
- (16) Puech, J.-L.; Feuillat, F.; Mosedale, J. R. *Am. J. Enol. Vitic.* **1999**, *50*, 469–478.
- (17) Marchal, A.; Cretin, B. N.; Sindt, L.; Waffo-Tégou, P.; Dubourdieu, D. *Tetrahedron* **2015**, *71*, 3148–3156.
- (18) Sindt, L.; Gammacurta, M.; Waffo-Tegou, P.; Dubourdieu, D.; Marchal, J. *Nat. Prod.* **2016**, *79*, 2432–2438.
- (19) Arramon, G.; Saucier, C.; Colombani, D.; Glories, Y. *Phytochem. Anal.* **2002**, *13*, 305–310.
- (20) Marchal, A.; Prida, A.; Dubourdieu, D. *J. Agric. Food Chem.* **2016**, *64*, 618–626.
- (21) Pompermaier, L.; Heiss, E. H.; Alilou, M.; Mayr, F.; Monizi, M.; Lautenschlaeger, T.; Schuster, D.; Schwaiger, S.; Stuppner, H. *J. Nat. Prod.* **2018**, *81*, 2091–2100.
- (22) Pérez, A. J.; Pecio, Ł.; Kowalczyk, M.; Kontek, R.; Gajek, G.; Stopinsek, L.; Mirt, I.; Oleszek, W.; Stochmal, A. *J. Agric. Food Chem.* **2017**, *65*, 4611–4623.
- (23) Subba Rao, G. S. R.; Prasanna, S.; Kumar, V. P. S.; Mallavarapu, G. R. *Phytochemistry* **1981**, *20*, 333–334.
- (24) Barua, A. D.; Pal, S. K.; Dutta, S. P. *J. Indian Chem. Soc.* **1972**, *5*, 519–520.
- (25) Bikas, C. P.; Achari, B.; Price, K. R. A. *Phytochemistry* **1991**, *30*, 4177–4179.
- (26) Muccilli, V.; Cardullo, N.; Spatafora, C.; Cunsolo, V.; Tringali, C. *Food Chem.* **2017**, *215*, 50–60.
- (27) Cretin, B. N.; Dubourdieu, D.; Marchal, A. *LWT - Food Sci. Technol.* **2018**, *87*, 61–66.
- (28) Gawel, R.; Sluyter, S. C. V.; Smith, P. A.; Waters, E. J. *Am. J. Enol. Vitic.* **2013**, *64*, 425–429.
- (29) Fischer, U.; Noble, A. C. *Am. J. Enol. Vitic.* **1994**, *45*, 6–10.

- (30) Furlan, A. L.; Jobin, M.-L.; Pianet, I.; Dufourc, E. J.; Géan, J. *Chem. Vine Wine Sci.* **2015**, *71*, 3143–3147.
- (31) Winstel, D.; Marchal, A. *Molecules* **2019**, *24*, 117.
- (32) Salagoity-Auguste, M.-H.; Tricard, C.; Sudraud, P. *J. Chromatogr. A* **1987**, *392*, 379–387.
- (33) Fayad, S.; Cretin, B. N.; Marchal, A. *Food Chem.* **2020**, *311*, 125881.
- (34) IOFI Working Group on Methods of Analysis. *Flavour Fragr. J.* **2010**, *25*, 2–3.
- (35) Prida, A.; Ducouso, A.; Petit, R. J.; Nepveu, G.; Puech, J.-L. *Ann. For. Sci.* **2007**, *64*, 313–320.
- (36) Prida, A.; Boulet, J.-C.; Ducouso, A.; Nepveu, G.; Puech, J.-L. *Ann. For. Sci.* **2006**, *63*, 415–424.
- (37) Cadahía, E.; Fernández de Simón, B.; Jalocho, J. *J. Agric. Food Chem.* **2003**, *51*, 5923–5932.
- (38) Chatonnet, P.; Boidron, J.-N.; Pons, M. *OENO One* **1989**, *23*, 223–250.
- (39) Gimenez Martinez, R.; Lopez Garcia De La Serrana, H.; Villalon Mir, M.; Quesada Granados, J.; Lopez Martinez, M. C. *Am. J. Enol. Vitic.* **1996**, *47*, 441–446.
- (40) Sarni, F.; Moutounet, M.; Puech, J.-L.; Rabier, P. *Holzforsch - Int. J. Biol. Chem. Phys. Technol. Wood* **2009**, *44*, 461–466.
- (41) Chatonnet, P.; Cutzach, I.; Pons, M.; Dubourdieu, D. *J. Agric. Food Chem.* **1999**, *47*, 4310–4318.
- (42) Glabasnia, A.; Hofmann, T. *J. Agric. Food Chem.* **2007**, *55*, 4109–4118.
- (43) Guichoux, E.; Garnier-Géré, P.; Lagache, L.; Lang, T.; Boury, C.; Petit, R. J. *Mol. Ecol.* **2013**, *22*, 450–462.

Table 1. ¹H NMR Assignments for Compounds 1–6 (600 MHz, MeOH-*d*₄)

position	1	2	3	4	5	6
	δ_{H} (<i>J</i> in Hz)	δ_{H} (<i>J</i> in Hz)	δ_{H} (<i>J</i> in Hz)	δ_{H} (<i>J</i> in Hz)	δ_{H} (<i>J</i> in Hz)	δ_{H} (<i>J</i> in Hz)
1 α	1.13 m	2.10 dd (12.6, 4.8)	0.90 m	0.90 m	0.90 m	0.89 m
1 β	2.11 td (12.5, 4.3)	1.08 m	2.06 dd (12.6, 5)	2.06 dd (12.6, 4.4)	2.06 dd (12.6, 4.4)	2.04 dd (12.9, 4.6)
2	4.36 td (10.3, 3.9)	4.59 td (9.9, 4.9)	4.41 m	4.42 m	4.42 m	4.45 m
3	5.20 d (9.9)	4.74 d (9.9)	3.12 d (9.9)	3.11 d (9.7)	3.11 d (9.7)	3.16 d (9.5)
4						
5	1.75 m	1.24 m	1.11 dd (12.1, 1.4)	1.11 m	1.11 m	1.11 m
6 α	1.74 m	1.71 m	1.67 m	1.67 m	1.67 m	1.70 m
6 β	1.79 m	1.86	1.85 m	1.83 m	1.83 m	1.80 m
7 α	1.32 m	1.56 td (12.9, 3.3)	1.33 m	1.36 m	1.36 m	1.35 m
7 β	1.60 m	1.36 m	1.49 m	1.48 m	1.48 m	1.47 m
8						
9	1.93 m	1.84 m	1.75 m	1.73 m	1.73 m	1.72 m
10						
11 α	2.01 m	2.03 m	1.96 m	1.98 m	1.98 m	1.98 m
11 β	2.06 m		2.03 m	2.03 m	2.03 m	2.00 m
12	5.35 brd	5.35 t (3.4)	5.34 t (3.4)	5.35 t (3.7)	5.35 t (3.7)	5.32 t (3.7)
13						
14						
15 α	1.03 m	1.06 m	1.01 m	1.01 m	1.01 m	1.00 m
15 β	1.76 m	1.67 m	1.63 m	1.65 m	1.65 m	1.64 m
16 α	1.63 m	1.63 m	1.66 m	1.74 m	1.74 m	1.70 m
16 β	2.31 td (12.8, 3.7)	2.32 td (13.8, 3.5)	2.30 td (12.7,3.2)	2.30 td (12.5, 3.4)	2.30 td (12.5, 3.4)	2.30 brd
17						
18	3.07 brd	3.08 brd	3.07 d (3.8)	3.07 d (3.8)	3.07 d (3.8)	3.05 brd
19	3.27 m	3.27 d (3.7)	3.29 d (3.8)	3.31 m	3.31 m	3.28 m
20						
21 α	1.06 m	1.76 m	1.02 m	1.02 m	1.02 m	1.02 m
21 β	1.75 m	1.03 m	1.79 m	1.79 m	1.79 m	1.81 m
22 α	1.63 m	1.64 m	1.63 m	1.66 m	1.66 m	1.67 m
22 β	1.78 m	1.78 m	1.79 m	1.80 m	1.80 m	1.82 m
23 α	3.26 m		1.52 s		1.52 s	
23 β	3.88 d (11.9)					
24	10.10 s	1.25 s		1.52 s		1.61 s
25	0.96 s	1.05 s	0.94 s	0.95 s	0.95 s	0.95 s
26	0.78 s	0.80 s	0.77 s	0.75 s	0.75 s	0.75 s
27	1.34 s	1.34 s	1.30 s	1.29 s	1.29 s	1.29 s

28						
29	0.95 s	0.95 s	0.96 s	0.97 s	0.97 s	0.95 s
30	0.96 s	0.97 s	0.97 s	0.97 s	0.97 s	0.95 s
1'			4.39 d (7.9)	5.38 d (8.4)	5.38 d (8.4)	5.38 d (8.1)
2'			3.36 m	3.34 m	3.34 m	3.32 m
3'			3.41 m	3.36 m	3.36 m	3.35 m
4'			3.46 m	3.38 m	3.38 m	3.36 m
5'			3.65 m	3.40 m	3.40 m	3.41 m
6' α			4.37 m	3.69 dd (4.4, 12.2)	3.69 dd (4.4, 12.2)	3.68 dd (4.3, 12.1)
6' β			4.62 dd (12.2, 2.1)	3.83 brd (12.2)	3.83 brd (12.2)	3.83 d (12.3)
1"				4.39 d (8.9)	4.39 d (8.9)	4.41 d (8.0)
2"				3.36 m	3.36 m	3.35 m
3"				3.42 m	3.42 m	3.42 m
4"				3.46 m	3.46 m	3.45 m
5"				3.65 m	3.65 m	3.65 m
6" α				4.39 m	4.39 m	4.36 m
6" β				4.62 dd (12.2, 2.1)	4.62 dd (12.2, 2.1)	4.60 brd
1'''						
2''', 6'''	7.08 s	7.14 s	7.13 s	7.12 s	7.12 s	7.12 s
3''', 5'''						
4'''						
7'''						

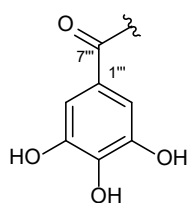
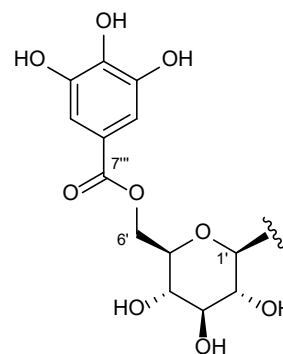
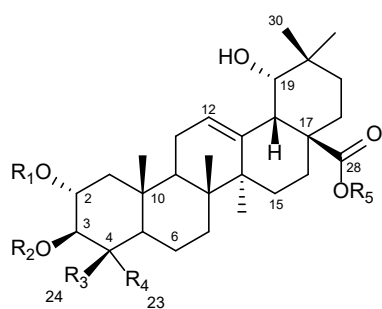
Table 2. ¹³C NMR Assignments for Compounds 1–6 (150 MHz, MeOH-*d*₄)

position	1	2	3	4	5	6
	δ_c , type	δ_c , type	δ_c , type	δ_c , type	δ_c , type	δ_c , type
1 α	46.2, CH ₂	47.5, CH ₂	46.3, CH ₂	46.1, CH ₂	46.7, CH ₂	45.2, CH ₂
1 β						
2	66.5, CH	65.8, CH	65.6, CH	65.5, CH	65.8, CH	65.1, CH
3	76.8, CH	82.8, CH	93.2, CH	93.1, CH	93.2, CH	93.5, CH
4	59.1, C	49.7, C	50.6, C	50.6, C	50.8, C	52.4, C
5	49.2, CH	56.1, CH	56.3, CH	55.9, CH	56.6, CH	55.6, CH
6 α	18.5, CH ₂	19.9, CH ₂	19.4, CH ₂	18.9, CH ₂	19.9, CH ₂	20.1, CH ₂
6 β						
7 α	32.0, CH ₂	32.4, CH ₂	32.1, CH ₂	31.9, CH ₂	32.4, CH ₂	32.9, CH ₂
7 β						
8	39.2, C	39.4, C	38.8, C	38.9, C	38.5, C	38.1, C
9	46.8, CH	47.6, CH	47.7, CH	47.0, CH	47.6, CH	47.6, CH
10	37.6, C	38.3, C	37.9, C	37.4, C	37.9, C	37.3, C
11 α	23.9, CH ₂	23.5, CH ₂	23.2, CH ₂	23.0, CH ₂	23.4, CH ₂	23.1, CH ₂
11 β						
12	124.6, CH	123.2, CH	123.5, CH	123.1, CH	123.5, CH	123.4, CH
13	143.3, C	143.2, C	143.1, C	143.5, C	142.7, C	142.7, C
14	41.3, C	41.3, C	41.5, C	41.10, C	40.4, C	40.5, C
15 α	28.2, CH ₂	27.9, CH ₂	26.9, CH ₂	27.6, CH ₂	28.0, CH ₂	27.3, CH ₂
15 β						
16 α	28.7, CH ₂	27.3, CH ₂	27.0, CH ₂	26.6, CH ₂	26.9, CH ₂	26.5, CH ₂
16 β						
17	45.4, C	45.2, C	45.6, C	45.0, C	45.7, C	45.5, C
18	43.8, CH	43.8, CH	44, CH	43.0, CH	43.7, CH	43.1, CH
19	81.1, CH	81.0, CH	81.1, CH	80.7, CH	80.7, CH	80.6, CH
20	34.5, C	34.4, C	34.6, C	34.4, C	34.4, C	34.3, C
21 α	28.2, CH ₂	28.0, CH ₂	27.7, CH ₂	27.5, CH ₂	28.1, CH ₂	28.2, CH ₂
21 β						
22 α	32.6, CH ₂	32.4, CH ₂	32.1, CH ₂	31.7, CH ₂	31.9, CH ₂	32.1, CH ₂
22 β						
23 α	58.3, CH ₂	175.8, C	22.2, CH	177.0, C	22.6, CH	174.4, C
23 β						
24	203.7, CH	23.2, CH	176.8, C	22.2, CH	176.9, C	24.2, CH
25	16.6, CH	13.5, CH	13.3, CH	12.9, CH	13.5, CH	13.4, CH
26	16.4, CH	16.1, CH	16.2, CH	15.5, CH	16.2, CH	15.2, CH
27	25.9, CH	23.5, CH	23.1, CH	22.8, CH	23.4, CH	23.1, CH
28	180.9, C	180.6, C	180.7, C	179.5, C	176.7, C	176.9, C
29	27.1, CH	27.1, CH	26.9, CH	26.7, CH	27.0, CH	27.0, CH
30	23.9, CH	23.8, CH	23.4, CH	23.2, CH	23.7, CH	23.0, CH
1'			105.2, CH	105.0, CH	94.2, CH	94.2, CH
2'			73.6, CH	73.2, CH	72.2, CH	72.8, CH
3'			76.6, CH	76.2, CH	77.2, CH	77.2, CH
4'			69.6, CH	69.6, CH	69.8, CH	70.0, CH
5'			74.4, CH	74.1, CH	77.0, CH	77.0, CH
6' α			62.3, CH ₂	62.5, CH ₂	61.1, CH ₂	60.4, CH ₂
6' β						
1''					105.2, CH	104.9, CH
2''					73.6, CH	73.7, CH
3''					76.6, CH	76.8, CH
4''					69.6, CH	70.0, CH
5''					74.5, CH	74.4, CH
6'' α					62.7, CH ₂	63.0, CH ₂
6'' β						
1'''	120.1, C	120.7, C	119.8, C	120.9, C	119.8, C	119.7, C
2''', 6'''	109.0, CH	109.3, CH	109.0, CH	108.9, CH	109.0, CH	109.0, CH
3''', 5'''	145.2, C	144.8, C	145.0, C	145.6, C	144.8, CH	145.1, CH
4'''	138.5, C	138.2, C	138.6, C	138.8, C	138.5, CH	138.3, CH
7'''	167.1, C	167.6, C	166.4, C	166.8, C	166.8, CH	166.7, CH

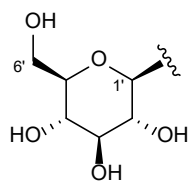
Table 3. Sensory Description of Isolated Compounds in Water and Non-Oaked White Wine

compound	taste intensity			
	water	white wine		
	bitterness	bitterness	acidity	sweetness
control	-	1	5	1
Glu-BA	1	3	4	1
1	1	2	3	2
2	3	5	3	1
3	0	1	4	1
4	0	3	3	1
5	4	5	3	1
6	4	5	4	1
7	2	5	5	1
8	0	2	3	3
9	2	4	3	1
10	0	2	4	1
11	2	3	2	1
12	2	4	4	1
13	2	2	2	3

Chart 1. Structures of Isolated Compounds



Gall = galloyl



Glc = glucosyl

Glc-Gall

compound	R ₁	R ₂	R ₃	R ₄	R ₅
1	H	Gall	CHO	CH ₂ OH	H
2	H	Gall	CH ₃	COOH	H
3	H	Glc-Gall	COOH	CH ₃	H
4	H	Glc-Gall	CH ₃	COOH	H
5	H	Glc-Gall	COOH	CH ₃	Glc
6	H	Glc-Gall	CH ₃	COOH	Glc
7	H	H	CH ₃	COOH	H
8	H	H	COOH	CH ₃	H
9	H	H	CH ₃	COOH	Glc
10	H	H	CHO	CH ₂ OGall	H
11	Gall	H	COOH	CH ₃	H
12	H	Gall	COOH	CH ₃	Glc
13	Gall	H	COOH	CH ₃	Glc
Glu-BA	H	H	COOH	CH ₃	Glc

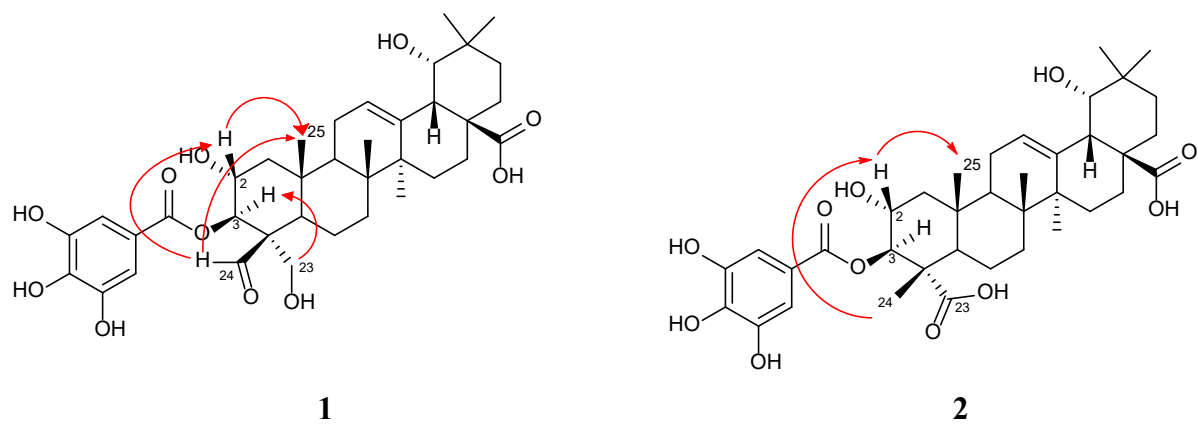


Figure 1. Selected ROESY correlations of compounds **1** and **2**.

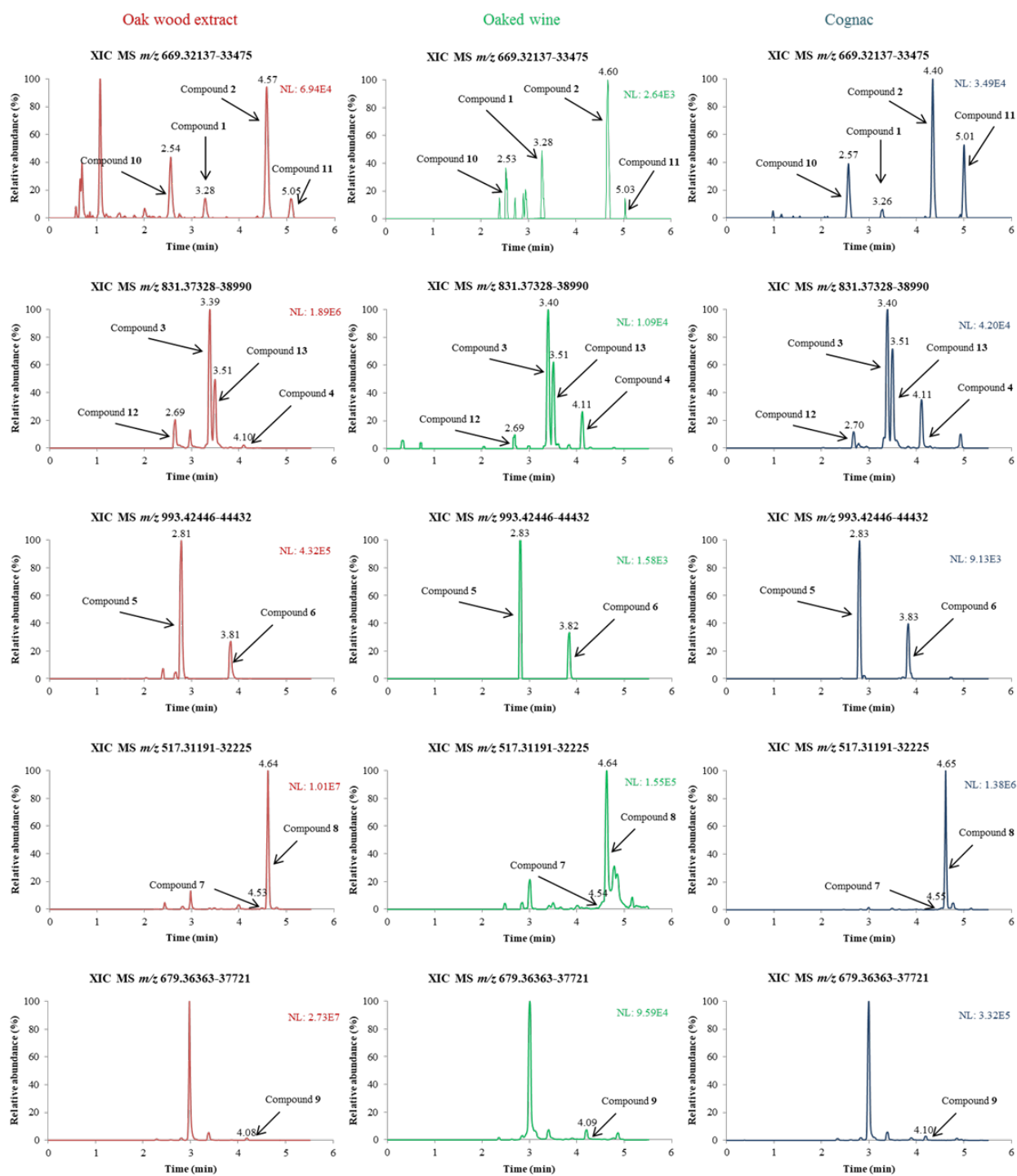


Figure 2. Negative LC-HRESIMS extracted ion chromatograms of an oak wood extract, an oaked wine, and a cognac (left to right) corresponding to $[M - H]^-$ ions of compounds 1 to 13 (top to bottom).

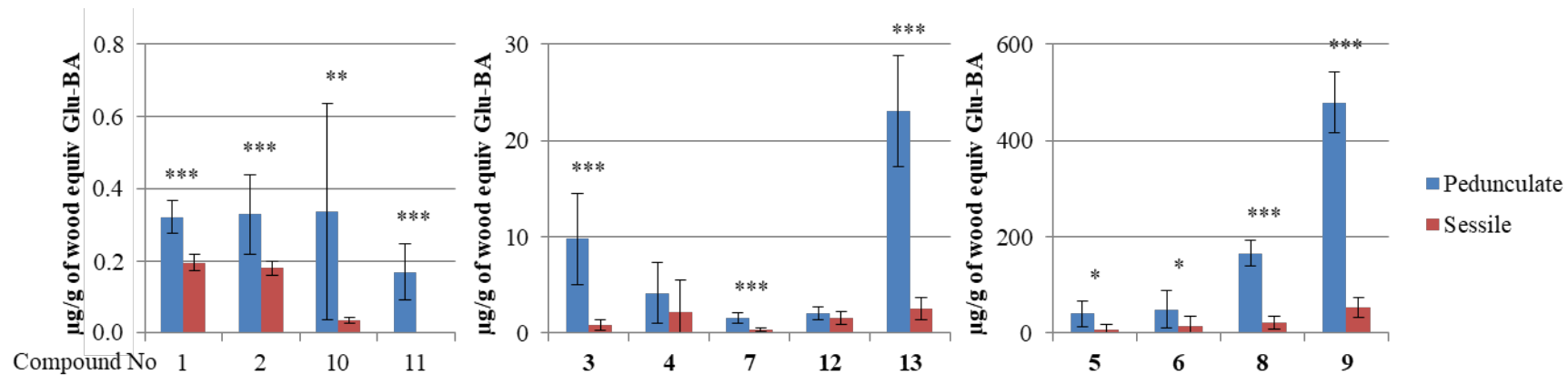


Figure 3. Concentrations (in µg/g equiv. Glu-BA) of compounds **1** to **13** in pedunculate and sessile oak wood extracts. Data are means ± CI, $n = 34$ for pedunculate oak wood, $n = 35$ for sessile oak wood. * $p < 0.05$, ** $p < 0.01$ and *** $p < 0.001$, Kruskal–Wallis test.

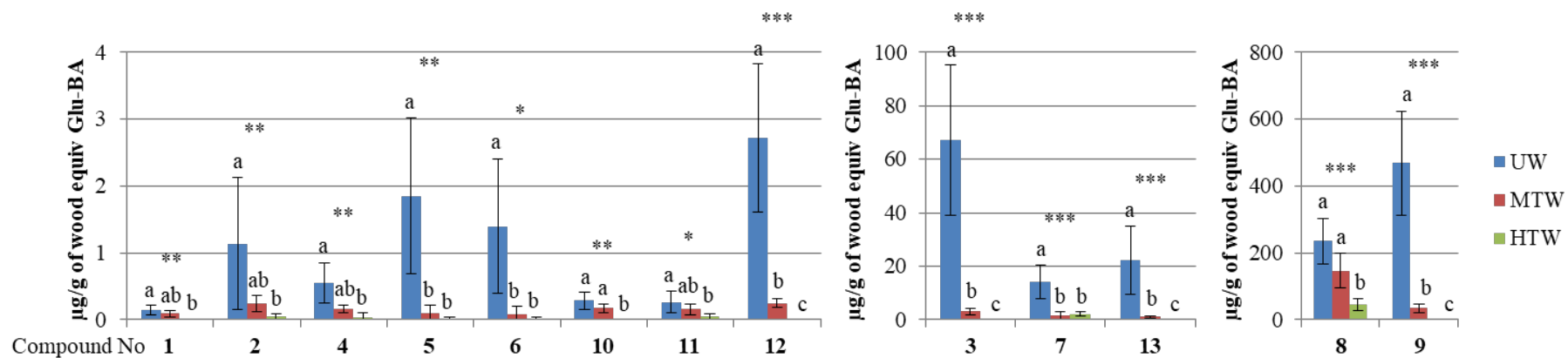


Figure 4. Concentrations (in µg/g equiv. Glu-BA) of compounds **1** to **13** in untoasted (UW), medium-toasted (MTW), and highly toasted (HTW) pedunculate oak wood extracts. Data are means ± CI, $n = 10$ for each modality. * $p < 0.05$, ** $p < 0.01$ and *** $p < 0.001$, Kruskal–Wallis test. Alphabetical letters indicate significant differences, post hoc Dunn test.

For TOC Graphic only

